Published in final edited form as:
Crit Care Med. 2011 December ; 39(12): 2711–2721. doi:10.1097/CCM.0b013e3182284a5f.

Induction of cellular antioxidant defense by amifostine improves ventilator induced lung injury

Panfeng Fu, PhD[1], **Jeffrey S. Murley, PhD**[2], **David J. Grdina, PhD**[2], **Anna A Birukova, MD**[1], and **Konstantin G. Birukov, MD, PhD**[1]

[1]Section of Pulmonary and Critical Care, Lung Injury Center, Department of Medicine, University of Chicago, IL, 60637 USA

[2]Department of Radiation and Cellular Oncology, University of Chicago, IL, 60637 USA

Abstract

Objective—To test the hypothesis that preconditioning animals with amifostine improves ventilator induced lung injury via induction of antioxidant defense enzymes. Mechanical ventilation at high tidal volume (HTV) induces reactive oxygen species (ROS) production and oxidative stress in the lung, which plays a major role in the pathogenesis of VILI. Amifostine attenuates oxidative stress and improves LPS-induced lung injury by acting as a direct scavenger of reactive oxygen and nitrogen species. This study tested effects of chronic amifostine administration on parameters of oxidative stress, lung barrier function and inflammation associated with ventilator induced lung injury.

Design—Randomized and controlled laboratory investigation in mice and cell culture.

Setting—University laboratory.

Subjects—C57BL/6J mice.

Interventions—Mice received once-daily dosing with amifostine (10-100 mg/kg, intraperitoneal injection) 3 days consecutively prior to HTV ventilation (30 ml/kg, 4 hrs) at day 4. Pulmonary endothelial cell (EC) cultures were exposed to pathological cyclic stretching (18% equibiaxial stretch) and thrombin in a previously-verified two-hit model of in vitro VILI.

Measurements and Main Results—Three-day amifostine preconditioning prior to HTV: 1) attenuated HTV-induced protein and cell accumulation in the alveolar space judged by BALF analysis; 2) decreased Evans Blue dye extravasation into the lung parenchyma; 3) decreased biochemical parameters of HTV-induced tissue oxidative stress; and 4) inhibited HTV-induced activation of redox-sensitive stress kinases and NF-κB inflammatory cascade. These protective effects of amifostine were associated with increased superoxide dismutase 2 (SOD2) expression and increased SOD and catalase enzymatic activities in the animal and endothelial cell culture models of VILI.

Correspondence: Konstantin G. Birukov, Director of Lung Injury Center, Section of Pulmonary and Critical Care, Department of Medicine, University of Chicago, 5841 S. Maryland Ave., MC 6026, Office N-611, Chicago, IL 60637, Phone: (773) 834-2636, Fax: (773) 834-2683, kbirukov@medicine.bsd.uchicago.edu.

The authors have not disclosed any potential conflicts of interest.

Conclusions—Amifostine preconditioning activates lung tissue antioxidant cell defense mechanisms and may be a promising strategy for alleviation of VILI in critically ill patients subjected to extended mechanical ventilation.

Keywords

Ventilator-induced lung injury; Amifostine; Endothelium; Reactive oxygen species; Superoxide dismutase 2

Introduction

Acute lung injury (ALI) is a devastating clinical syndrome characterized by severe lung inflammation and vascular barrier disruption that affects more than 200,000 patients per year in the US and is associated with a mortality rate of 30% to 50% [1, 2]. Mechanical ventilation remains an imperative treatment for ALI, especially for the patients with acute respiratory distress syndrome (ARDS). However, mechanical ventilation, particularly with high tidal volumes (HTV), can worsen or even cause *de novo* lung injury [3-8]. Despite recent advances in low tidal volume ventilator strategies and a better understanding of the underlying inflammatory pathophysiology of ALI, there remain few effective treatments for this devastating illness. Redox imbalance and lung oxidative damage contributes to various pathologic conditions including septic inflammation and ventilator-induced lung injury (VILI). Exacerbation of pre-existing lung injury by excessive mechanical ventilation worsens lung damage and increases associated oxidative stress, which remains a serious concern in defining optimal ventilation strategies. This study examined the role of amifostine preconditioning in the attenuation of oxidative damage in a simplified model of lung injury induced by high tidal volume mechanical ventilation alone.

Reactive oxygen species (ROS) and reactive nitrogen species (RNS) are important factors which exacerbate various pathological conditions, such as ARDS, sepsis, and ALI [9, 10]. Excessive mechanical stretch of lung tissue associated with high tidal volume mechanical ventilation induces intracellular oxidative stress by several mechanisms including induction of mitochondrial systems [11], activation of NADPH oxidase [12], or xanthine oxidoreductase [13]. *In vitro*, cyclic stretch triggers ROS production in lung epithelial and endothelial cells as early as 30 min after exposure [11, 14-16], suggesting that ROS induced by mechanical ventilation is an early event in the pathogenesis of ventilator-induced lung injury (VILI) [10, 17]. Consistent with this *in vitro* evidence, a redox imbalance has been observed in lungs exposed to mechanical ventilation [18]. Lung cells counteract the oxidative stress induced by various stimuli by employing a variety of antioxidant defense mechanisms. Manganese superoxide dismutase (SOD2) and catalase are effective endogenous antioxidant enzymes. SOD2, an inducible antioxidant enzyme located in the mitochondria, converts superoxide anion into hydrogen peroxide followed by the subsequent conversion of hydrogen peroxide into H_2O by catalase. The pathologic role of superoxide anion and high hydrogen peroxide levels has been well documented. Impairment of SOD2 has been related to asthma pathophysiology [19], decreased pulmonary radiation resistance [20], and increased sensitivity to oxygen toxicity [21]. Likewise, catalase also plays an important role in lung diseases. Mitochondrial localization of catalase attenuates H_2O_2-induced lung epithelial cell death [22], and targeting of catalase to the endothelium, using catalase conjugated to an ACE antibody, attenuates ischemia-reperfusion injury of the lung *in vivo* [23]. Thus, therapeutic strategies aimed at the upregulation of antioxidant defense enzymes may be beneficial for the treatment of pathologic conditions associated with oxidative stress including VILI.

Amifostine (S-2[3-aminopropylamino]-ethylphosphorothioic acid, WR-2721) is a phosphorothioate that is converted to its active free thiol form through dephosphorylation by alkaline phosphatase in tissue [24]. It is currently the only radioprotective drug approved by the United States Food and Drug Administration (FDA) for use as a cytoprotective agent to decrease the incidence of moderate-to-severe xerostomia in patients undergoing postoperative radiation therapy for the treatment of head-and-neck cancer [25]. Our previous study demonstrated the protective effect of a single amifostine administration in LPS-induced acute lung injury through a direct free radical scavenging effect [26]. In addition to the immediate amifostine antioxidant effects due to free oxygen radical scavenging, amifostine exhibits additional activities. For example, daily administration of amifostine for 3 days caused a 20-40% increase in cellular radiation resistance in animals exposed to ionizing radiation [27]. Another study shows improvement of hemodynamic parameters in rat models of doxorubicin induced cardiotoxicity, where amifostine was chronically administered at doses up to 75 mg/kg [28].

In this study we investigated the effect of daily administration of amifostine during 3 consecutive days prior to mechanical ventilation on the development of VILI and examined stress-induced pathways, levels of SOD2 and catalase expression and enzymatic activity as potential molecular mechanisms underlying the protective effects of chronic amifostine preconditioning.

Results

Preconditioning with amifostine attenuates VILI and lung vascular permeability

HTV significantly elevated BAL inflammatory cell counts. This effect was markedly attenuated by three-day amifostine pre-treatment at 25 mg/kg, 50 mg/kg, and 100 mg/kg (42%, 33% and 25%, respectively) (Figure 1A), while amifostine treatment at 10 mg/kg was not effective. Likewise, HTV caused significant barrier disruption, inducing an increase in BAL protein compared with vehicle control. This effect was significantly attenuated by triple daily amifostine treatment at 25 mg/kg and 50 mg/kg, but not at 10 mg/ml and 100 mg/ml doses (Figure 1B). The protective effects of amifostine against vascular leak were further assessed by measurement of Evans blue leakage into the lung tissue. The amifostine dose causing the maximal protective effect (25 mg/kg) was used in these experiments. HTV induced noticeable Evans blue leakage from the vascular space into the lung parenchyma, which was significantly decreased by amifostine pretreatment (Figure 2A). These results were confirmed by quantitative analysis of Evans blue-labeled albumin accumulation in the lung tissue sample (Figure 2B). Histological analysis of lung sections revealed lung recruitment of inflammatory cells and areas of alveolar hemorrhage indicative of vascular disruption with HTV ventilation (control 5.9±1.7 cells/field; amifostine alone 5.7±1.6 cells/field vs 48.8±9.0 cells/field for HTV; $p<0.01$). These effects were attenuated by amifostine (14.2±2.9 cells/field; $p<0.01$ vs HTV) (Figure 2B). These results strongly suggest that amifostine preconditioning has a protective effect for HTV-induced lung injury.

Amifostine attenuates oxidative stress induced by HTV

HTV increased lung tissue MDA content, and this increase was attenuated by amifostine (Figure 3A). HTV also enhanced nitrotyrosine accumulation in the lung tissue, which was attenuated by amifostine pretreatment (Figure 3B). Similar results were obtained by analysis of oxidized proteins. Western blot analysis of lung tissue homogenates demonstrated that HTV induced a significant increase in oxidized proteins compared to vehicle control animals, which was attenuated by 25 mg/kg amifostine treatment (Figure 3C). These data together show that three parameters reflecting oxidative stress in ventilated lungs are suppressed by amifostine.

Amifostine attenuates HTV-induced oxidative-sensitive signaling pathways

HTV increased p38, JNK and Erk1/2 phosphorylation as determined by western blot analysis of lung tissue samples with corresponding phospho-specific antibodies. Amifostine pretreatment significantly attenuated HTV-induced phosphorylation of p38 and JNK MAP kinases, but did not affect Erk1/2 (Figure 4).

The significant Evans blue accumulation in lung tissue caused by HTV as described above, suggests impaired lung vascular barrier function. Therefore, we next analyzed the effects of HTV and amifostine treatment on the activation of cytoskeletal proteins regulating vascular permeability. Our data demonstrate that HTV induced MYPT phosphorylation at Thr850 and MLC phosphorylation in lungs, and that these signaling events were markedly suppressed by amifostine treatment (Figure 4).

HTV induced a marked degradation of IκB, which was blocked by amifostine preconditioning (Figure 4).

Effects of amifostine on SOD2 and catalase enzymatic activity

Chronic preconditioning of mice with amifostine in the 50 - 100 mg/kg range increased SOD2 enzymatic activity in the homogenized lung tissue samples (Figure 5A), while short-term treatment with amifostine (100 mg/kg; 30 min) had no effect on SOD2 activity (data not shown). HTV had no effect on basal SOD2 activity in the lungs of untreated mice (Figure 5A).

Analysis of catalase activity showed that, in contrast to the effects on induction of SOD2, amifostine preconditioning did not increase catalase activity in non-ventilated mice (Figure 5B). Interestingly, exposure to HTV decreased catalase activity in the lungs of vehicle-treated mice. Despite apparently elevated levels of catalase activity in (HTV + Amifostine) group, the difference between this and HTV groups was not statistically significant ($p=0.54$). Of note, catalase activity in (HTV + Amifostine) group corresponded to amifostine-treated non-ventilated mice. Western blot analysis showed a significant increase in SOD2 protein content in the lungs of amifostine-preconditioned mice, while catalase protein levels remained unchanged (Figure 5C).

The SOD inhibitor DECT blocks suppression of HTV-induced inflammatory cell and protein accumulation in BAL samples from mice preconditioned with amifostine

The role of SOD activity for amifostine's protective effects against VILI was further tested in experiments with the pharmacological SOD inhibitor DECT. DECT blocked completely the amifostine preconditioning caused reduction of HTV-induced inflammatory cell and protein accumulation in BAL samples (Figure 6A). Abrogation of the amifostine-induced lung protective effects by DECT was also associated with the re-emergence of p38 MAP kinase activation and degradation of the NFκB subunit IκBα (Figure 6B).

Amifostine inhibits ROS production and inflammatory signaling by pulmonary endothelial cells in the in vitro two-hit model of VILI

We have previously described an *in vitro* two-hit model of VILI [37, 38] to directly test the effect of pathologically relevant cyclic stretch (18% CS) and barrier-disruptive agonists on ROS production in pulmonary endothelial cells. Thrombin alone caused a slight but significant increase in ROS production, while 18% CS induced a more robust ROS production. The combination of 18% CS and thrombin induced the largest increase in ROS (Figure 7A and B). EC preconditioning with amifostine prior to CS and thrombin stimulation dramatically inhibited ROS generation in response to combined CS and thrombin. Because amifostine was not present in the medium during the combined CS and

thrombin challenge, these data exclude the effects of amifostine as a direct ROS scavenger and strongly suggest an additional mechanism of action.

Amifostine enhances SOD2 activity in human pulmonary artery endothelial cells (HPAEC)

Chronic HPAEC preconditioning with 0.5 mM and 1.0 mM amifostine enhanced SOD2 activity in both control cells and cells exposed to pathologic CS and thrombin (Figure 8). Thrombin alone had no effect on SOD2 activity as compared to vehicle control. Cyclic stretch caused a decrease in SOD2 activity, compared with vehicle control cells, however the mean value did not reach significance (n=3, p=0.055).

Involvement of oxidative stress sensitive signaling pathways in response to cyclic stretch and HTV

Similar to our *in vivo* results (Figure 4), EC stimulation with 18% CS and thrombin increased phosphorylation of p38, JNK and Erk1/2 MAP kinases, increased phosphorylation of MYPT, MLC, and the p38 cytoskeletal target HSP-27, and also caused degradation of IκBα (Figure 9A). The combination of 18% CS and thrombin addition exhibited synergistic effects on the phosphorylation of p38, JNK, MYPT and MLC, while pretreatment with amifostine markedly attenuated these signaling events. Unlike p38 and JNK MAP kinases, amifostine did not attenuate phosphorylation of Erk1/2 induced by thrombin, CS, or their combination. In agreement with the effects observed *in vivo*, chronic preconditioning of human pulmonary EC cultures with amifostine significantly increased SOD2 protein expression (Figure 9B).

Discussion

Pathologic mechanical stress associated with mechanical ventilation at high tidal volume leads to elevated ROS production by lung cells, and the impact of oxidative stress in the pathogenesis of VILI has become well recognized [39]. Excessive activation of redox-sensitive signaling leads to further vascular barrier dysfunction culminating in pulmonary edema and acute lung injury [40, 41]. However, therapeutic approaches to enhance antioxidant defense mechanisms in ALI/ARDS patients have yet to be developed.

This study shows for the first time, that chronic amifostine preconditioning attenuates ventilator induced lung injury and suppresses associated inflammatory and barrier disruptive signaling pathways. The major finding of this work is the novel protective mechanism of amifostine preconditioning against HTV-induced lung oxidative stress and associated barrier dysfunction via induction of SOD expression and SOD/catalase activity.

Several factors contribute to stretch-induced ROS generation in lung cells including increased NADPH oxidase activity, and mitochondrial malfunction that leads to uncontrolled superoxide production, which may cause severe cellular oxidative stress [11, 14, 39, 42, 43]. HTV-induced lung dysfunction in this study was accompanied by lung tissue oxidative stress manifested by an increase in the protein nitrotyrosinylation and oxidation levels and elevated MDA levels in the lung tissue homogenates. *In vitro* experiments showed stretch-induced ROS production as early as 30 min after exposure to lung epithelial and endothelial cells [11, 14], suggesting direct ROS involvement in the pathogenesis of VILI.

Our data show HTV-induced the activation of the MAP kinases p38, Erk-1/2, JNK, NFkB cascade, and activation of Rho-dependent MLC phosphorylation, that was linked to increased lung vascular endothelial permeability [44-46]. In agreement with redox-dependent activation of stress-induced MAP kinase and NFκB signaling, these pathways were markedly suppressed by amifostine preconditioning and strongly correlated with

attenuation of HTV-induced lung injury. The results also demonstrate that HTV-induced Erk 1/2 activation was not suppressed by amifostine. Because amifostine only partially attenuated barrier dysfunction, it is possible that Erk 1/2 may be involved in other mechanisms contributing to barrier dysfunction. A protective effect of amifostine on stress kinase and Rho pathways involved in lung barrier dysfunction were also observed in the cell culture two-hit model of VILI.

Amifostine is rapidly cleared from the bloodstream, as evidenced by a 10-fold drop in concentration within 30 min of injection in mice [47]. In this study the last amifostine injection was 24 hrs prior to HTV experiments, indicating the likelihood that amifostine had been cleared from the circulation well before the onset of experiments. Thus, the observed protective effects were attributed to a delayed, rather than, immediate amifostine action.

Our previous study [26] described the protective effects of amifostine treatment concurrent with intratracheal LPS instillation in an animal model of LPS-induced lung injury. Amifostine is effective in scavenging highly reactive free radicals by its active free thiol groups, and the mechanism underlying the protective effect of amifostine in that model was due to its capacity to scavenge excessive reactive free radicals generated in response to LPS stimulation. A number of reports, however, indicate that amifostine may increase cell resistance to radiation-induced death by a delayed mechanism via induction of SOD2 gene expression and enzymatic activity [48-50]. The same mechanism may cause the observed amifostine-induced lung protection in VILI, as our data show increased expression of SOD in the lung samples and pulmonary endothelial cell cultures after 3 days of preconditioning with amifostine. This effect was not observed at earlier times (2 hrs) of amifostine pretreatment (data not shown).

It is important to note that, in contrast to the reported protective effects of acute amifostine treatment in the model of LPS-induced lung injury, where the maximal amifostine protective effect was observed at 200 mg/kg [26], maximal protection by chronic pretreatment performed in this study was observed at a significantly lower dose (25 mg/kg). A key role of SOD2 in the amifostine-induced protective effects observed in the VILI model was demonstrated also in these experiments, with the introduction of the SOD2 pharmacological inhibitor DECT.

Inducible SOD2 expression is regulated by two transcription factors, NFκB [51] and the Forkhead Box O3a transcription factor (FOXO3a) [52]. Activation of the SOD2 gene expression can also be induced by thiol reducing agents, such as amifostine and has been described as the thiol-induced SOD2-mediated “delayed radioprotective effect” [53] [49]. Amifostine-triggered cellular activation of NFκB leads to elevated SOD2 gene expression and a 10-to 20-fold buildup of active SOD2 enzyme, which peaks about 24 to 30 h later [49, 50]. The proposed mechanism of such NFκB activation is via reduction of cysteine residues on the p50 and p65 subunits of NFκB that results in its activation and enhanced binding to the NFκB binding site(s) of the SOD2 gene [54]. This in turn induces SOD2 gene expression and translocation of active SOD2 enzyme to the mitochondria.

Activation of NFκB by amifostine results in selective rather than global changes in the expression of genes containing NFκB-responsive elements [55]. This observation and the transient nature of NFκB activation may explain the apparent discrepancy between NFkB-dependent activation of SOD2 and inhibition of VILI-induced NFkB activation in amifostine-preconditioned lungs, which is due to SOD2-mediated reduction of oxidative stress and redox-dependent NFκB and stress kinase signaling.

Previous studies show that amifostine at a 50 mg/kg dose was also more effective than a 200 mg/kg dose in inhibiting metastases formation [56] and was more effective in inducing the

conversion of plasminogen to angiostatin. Such bell-shaped dose responses are expected in the case of a reduction/oxidation (redox) driven reaction, where each SH moiety is considered as a reducing equivalent. Thus, at certain concentrations, redox states reach a plateau level, and further increases may cause adverse reactions. For example, amifostine triggers hypoxic signaling [57], which at high doses may impair its beneficial effects in the VILI model. Amifostine treatment also down-regulated VEGFR-2 expression in endothelial cells and suppressed their ability to respond to exogenous VEGF-A [58]. VEGF signaling plays a complex role in the pathogenesis of ALI. At high concentrations, VEGF promotes vascular dysfunction, while basal levels are essential for endothelial and alveolar epithelial cell survival [59, 60]. Thus, imbalances between the beneficial activation of antioxidant defenses shown in the present study, and desensitization of VEGF signaling contributing to the development of ALI, may be a potential explanation of the decreased amifostine efficacy at higher concentrations.

Consistent with previous reports [27], chronic amifostine treatment did not upregulate catalase protein expression or enzymatic activity in the lung tissues or cultured pulmonary EC. However, amifostine pretreatment prevented a drop in catalase activity observed in the lungs of animals ventilated at high tidal volumes. The mechanism of this inhibitory effect is not entirely clear. Since catalase transcriptional activation is not regulated by amifostine, the most plausible explanation of preserved catalase activity in the lungs of HTV-exposed amifostine-preconditioned mice is due to the prevention of oxidative stress-induced posttranslational modification(s) that may lead to catalase inactivation. Figure 10 summarizes the major findings of this study and proposes a mechanism explaining the delayed amifostine protective effects in ventilator induced lung injury. Chronic treatment with amifostine causes induction of SOD2 protein expression and enzymatic activation of SOD2 and catalase, which in turn suppresses HTV-induced ROS and RNS production, mitigates oxidative stress, and inhibits redox-sensitive stress signaling involved in inflammatory gene expression and barrier disruptive mechanisms in the lung.

VILI is a multi-facet pathologic condition involving multiple pathologic mechanisms. Excessive cyclic stretch of the lung associated with VILI may directly disrupt the plasma membrane [61, 62], cause release and *de novo* production of inflammatory cytokines (IL-8, TNFα) and coagulation factors (TF, thrombin) leading to vascular hyperpermeability and lung dysfunction [62-64]. In addition, VILI-associated activation of surface adhesive molecules (ICAM-1, VCAM) [65-67] triggers neutrophil adhesion and infiltration into the lungs. Excessive mechanical stretch associated with VILI induces signal transduction triggered by MLCK and RhoGTPase dependent mechanisms and leads to EC cytoskeletal remodeling and permeability [35, 38]. Various strategies to reduce MLCK or Rho signaling show promising results in the *in vitro* and *in vivo* models of VILI [6, 29, 30, 38, 68]. In addition to the MLCK- and Rho-dependent mechanisms of lung barrier dysfunction, this study and other reports describe direct activation of ROS production and oxidative stress in VILI or pathologic CS *in vitro* [39, 42, 69]. Such oxidative stress activates cellular stress signaling and has been implicated in disruption of cell junction integrity, activation of cytoskeletal contractile machinery, and production of inflammatory mediators, which further exacerbate lung dysfunction. The results of this study and published data [39] suggest that the reduction of oxidative stress may be a promising strategy to suppress pathologic signaling in VILI. Thus, simultaneous targeting of several pathogenic mechanisms including oxidative stress (by amifostine), thrombin-induced procoagulant activities and increased vascular permeability (by treatment with activated protein C), downregulation of mechanical stress- and agonist-induced Rho signaling via elevation of intracellular cAMP [68], regulation of microtubule dynamics [30], or stimulation of Rac/Cdc42 signaling [70, 71] may prove to be efficient strategies to prevent or cure this devastating pathologic condition.

CONCLUSIONS

The results of this study strongly suggest that chronic amifostine treatment may reduce pathologic ROS production in the clinical setting associated with acute lung injury and may be considered as a preventive treatment for a wider spectrum of ALI syndromes associated with pathologic elevation of ROS production and oxidative stress. Although rigorous testing of various protocols of amifostine administration are still required, our results suggest that amifostine-mediated induction of cellular antioxidant defense mechanisms may be also beneficial at advanced ALI stages and improve resolution of ALI/VILI. These are important directions for future studies.

Materials and Methods

Reagents and cell culture

Amifostine (free thiol compound WR-1065 used *for in vitro* and prodrug formulation WR-2721 used *in vivo*) were obtained from the Drug Synthesis and Chemistry Branch, Division of Cancer Treatment, National Cancer Institute. Nitrotyrosine antibody was purchased from Invitrogen (San Francisco, CA); antibodies against phosphorylated myosin light chain (MLC), p38, JNK1/2, and Erk1/2 MAP kinases, heat shock protein 27 (Hsp27), IκBα, and NFκB-p65 were obtained from Cell Signaling (Beverly, MA). Image-iT LIVE green reactive oxygen species detection kit was purchased from Molecular Probes, Inc., (Eugene, OR). SOD and Catalase Assay Kit were purchased from Cayman Chemical Company (Ann Arbor, MI). Malondialdehyde (MDA) Assay Kit was from OXISResearch (Foster City, CA). OxyBlot Protein Oxidation Detection Kit and phospho-specific antibody to MLC protein phosphatase 1 (MYPT1) were from Millipore (Billerica, MA).

In vivo model of VILI

All animal care and treatment procedures were approved by the University of Chicago Institutional Animal Care and Use Committee and were handled according to the National Institutes of Health Guide for the Care and Use of Laboratory Animals. Adult male C57BL/6J mice, 8-10 week old, with average weight 20-25 grams (Jackson Laboratories, Bar Harbor, ME) were housed in pathogen-free conditions in the University of Chicago Animal Care Facilities. Mice were intraperitoneally (i.p.) treated with WR2721 at 4 different doses (10 mg/kg, 25 mg/kg, 50 mg/kg, and 100 mg/kg) or PBS as control daily for 3 days. On day 4, mice were anesthetized with an intraperitoneal injection of ketamine (75 mg/kg) and acepromazine (1.5 mg/kg). The intensity of anesthesia was monitored by toe pinch using tweezers. When a sharp withdrawal of the hind leg was observed after the toe was pinched, an additional i.p. bolus of the anesthetic mixture was applied. Tracheotomy was performed, and the trachea was cannulated with a 20-G intravenous catheter through the mouth. Ventilation was performed at tidal volume of 30 ml/kg, 75 breaths per minute, 0 PEEP for 4 hours. Non-ventilated animals injected with vehicle (PBS) or amifostine (i.p.) were used as controls. In order to maintain arterial blood pressure in the normal range, mice received i.p. boluses 0.1 ml/hr of phosphate buffered saline. In experiments with DETC control and amifostine-preconditioned mice were injected with DECT (3 mg/kg, i.v.) 30 min before the onset of ventilation. At the end of the experiment, BAL was performed using 1 ml of warmed sterile Hanks Balanced Salt Buffer (+30°C). The collected lavage fluid was centrifuged at 2500 rpm for 20 min at +4°C; the supernatant was removed and frozen at −80°C for subsequent protein study. BAL inflammatory cell counting was performed using a standard hemocytometer technique. The BAL protein concentration was determined by BCATM Protein Assay kit (Superscript).

Assessment of pulmonary vascular leakage by Evans blue

Evans blue dye (EBD, 30 ml/kg) was injected into the external jugular vein 2 hrs before termination of experiment to assess vascular leak. At the end of experiment, thoracotomy was performed, and the lungs were perfused in-situ via left atrium with PBS containing 5 mM EDTA to flush the blood off the lungs. Left lung and right lungs were excised and imaged by Kodak digital camera. After imaging, lungs were blotted dry, weighed and homogenized in PBS (1 ml/100 μg tissue) and used for quantitative analysis of EB tissue accumulation. Briefly, homogenized tissue was incubated with 2 volumes of formamide (18 h, 60°C) and centrifuged at 12,000 g for 20 min. Optical density of the supernatant was determined by spectrophotometry at 620 nm and 740 nm. EBD concentration in the lung tissue homogenates (μg Evans blue dye/g tissue) was calculated against a standard curve.

Histological assessment of lung injury

Left lungs were intratracheally instilled with 10% formalin from 20 cm height, immersed in 10% formalin for at least 24 hours and then embedded in paraffin. After deparaffinization and dehydration, the lungs were cut into 4-μm sections, and stained with hematoxylin and eosin. Alveolar fluid accumulation and neutrophil infiltration as indices of lung leak and inflammation were evaluated by bright field microscopy of lung tissue sections at × 40 magnification. Leukocyte infiltration was evaluated by counting leukocytes per microscopic field, ten fields per condition.

SOD, catalase enzyme activity, and MDA content assays

Protein extracts from lung tissue homogenates or cell culture were centrifuged at 10000 rpm for 20 min at 4 °C. Supernatant were taken for protein concentration measurement. The left samples were used for SOD, catalase and MDA measurement. SOD assay utilizes a tetrazolium salt for detection of superoxide radicals generated by xanthine oxidase and hypoxanthine. Reaction is initiated by adding xanthine oxidase to samples. After 20 min incubation at room temperature, absorbance was read at 450 nm. One unit of SOD is defined as the amount of enzyme need to exhibit 50% dismutation of the superoxide radical. Catalase assay is based on the reaction of catalase with methanol in the presence of an optimal concentration of H_2O_2. The formaldehyde produced is measured colorimetrically with 4-amino-3hydrazino-5-mercapto-1,2,4-triazole (purpald) as the chromogen. Purpald specifically forms a bicyclic heterocycle with aldehydes, which upon oxidation changes into a purple color. A 20 μl aliquot of homogenized lung tissue sample was incubated with 30 μl of methanol, and the reaction was initiated by adding 20 μl H_2O_2. After 20 min incubation 30 μl of potassium hydroxide was added to terminate the reaction and then add 30 μl of purpald followed by 10 min incubation. The absorbance was read at 540 nm, and catalase activity was calculated. One unit of catalase is defined as the amount of enzyme that will cause the formation of 1.0 nmol of formaldehyde per minute at 25 °C. MDA was measured based on the reaction of a chromogenic reagent, N-methyl-2-phenylindole (NMP1), with MDA at 45 °C. One molecule of MDA reacts with 2 molecules of NMP1 to yield a stable carbocyanine dye, which is readable at 586 nm. Contents were calculated against a standard curve.

Detection of oxidized proteins in lung tissue

Lung tissue protein oxidation was measured by the reaction converting carbonyl groups in the protein side chains into 2,4-dinitrophenylhydrazone (DNP-hydrazone). In brief, 15-20 μg of lung tissue protein was derivatized to DNP-hydrazone by reaction with 2,4 dinitrophenylhydrazine for 15 min at room temperature. The DNP-derivatized proteins were separated by SDS-PAGE gel electrophoresis followed by Western blotting with specific anti-DNP antibody.

Cell culture under cyclic stretch (CS)

All CS experiments were performed using an FX-4000T Flexercell Tension Plus system (Flexcell International Corporation, Hillsborough, NC, USA) equipped with a 25-mm BioFlex Loading Station as previously described. Experiments were performed in the presence of culture medium containing 2% fetal bovine serum. Briefly, ECs were seeded at standard densities (8×10^5 cells per well) onto collagen I-coated flexible-bottom BioFlex plates and treated daily with 0.5 mM or 1 mM amifostine. Medium was changed every day with fresh amifostine. After 72 hours of culture, each plate received fresh medium without amifostine supplied, was mounted onto the Flexercell system, and was exposed high-magnitude (18% elongation) CS to recapitulate the mechanical stresses experienced by the alveolar endothelium during normal respiration and HTV mechanical ventilation. Thrombin (0.02 U/ml) was added 15 min before termination of CS. Control BioFlex plates with static EC culture treated with thrombin were placed in the same cell culture incubator. At the end of experiment, cell lysates were collected for western blot, or CS-exposed endothelial monolayers were used for live ROS staining.

Detection of ROS production in live cells

ROS production was measured using Image-iT LIVE Green Reactive Oxygen Species Detection Kit (Molecular Probes, Inc., Eugene, OR, USA). In parallel, 3 days continuous 0.5 mM/ml or 1 mM/ml of amifostine-treated HPAEC cells were changed to medium without amifostine on the 4th day, and subjected to 18% CS or left as static control, 0.02 U/ml of thrombin was added to cell culture medium 15 min prior to the termination of stretch. At 2 hours, cells were washed in 37 °C Hanks buffer and incubated with 1 ml of 25 μM carboxy-H2DCFDA (ROS-activated fluorophor) working solution (25 min, 37 °C, protected from light). After 3-time wash in warm Hanks buffer cells were subjected to microscopy using Nikon video-imaging system (Nikon Inc, Tokyo, Japan) consisting of phase contrast inverted microscope equipped with set of objectives and filters for immunofluorescence and connected to a digital camera and image processor. Six fields were randomly chosen for each experiment condition. Mean fluorescence intensity was quantified by ImageJ software. The resulting fluorescence was expressed as folds to the mean intensity of vehicle control cells.

Western blot analysis

Protein extracts from mouse lungs or EC lysates were separated by SDS-PAGE and transferred onto nitrocellulose membranes followed by incubation with specific antibodies of interest. Equal protein loading was verified by re-probing of membranes with anti-β-tubulin antibody. Immunoreactive proteins were detected using the enhanced chemiluminescent detection system according to the manufacture's protocol (Amersham, Little Chalfont, UK). The relative intensities of immunoreactive protein bands (relative density units) were quantified by scanning densitometry using Image Quant software (Molecular Dynamics, Sunnyvale, CA). Densitometry results were expressed as a ratio of specific protein signal to β-tubulin signal.

Supplementary Material

Refer to Web version on PubMed Central for supplementary material.

Acknowledgments

Consultations on biostatistical data analysis of this study were supported by Grant UL1RR024999 from the National Center For Research Resources. The content is solely the responsibility of the authors and does not necessarily represent the official views of the National Center For Research Resources or the National Institutes of Health.

Supported by NIH grants NIH/NHLBI PO1-058064, HL076259, HL087823, ALA Career Investigator Award for KGB; NIH/NHLBI HL89257 for AAB; NIH/NCI RO1 CA99005 and DDE Grant DE-FG02-05ER64086 for DJG and JSM.

References

[1]. Rubenfeld GD, Caldwell E, Peabody E, Weaver J, Martin DP, Neff M, et al. Incidence and outcomes of acute lung injury. N Engl J Med. Oct 20; 2005 353(16):1685–93. [PubMed: 16236739]

[2]. Ware LB, Matthay MA. The acute respiratory distress syndrome. N Engl J Med. May 4; 2000 342(18):1334–49. [PubMed: 10793167]

[3]. Ranieri VM, Suter PM, Tortorella C, De Tullio R, Dayer JM, Brienza A, et al. Effect of mechanical ventilation on inflammatory mediators in patients with acute respiratory distress syndrome: a randomized controlled trial. Jama. Jul 7; 1999 282(1):54–61. [PubMed: 10404912]

[4]. Tremblay L, Valenza F, Ribeiro SP, Li J, Slutsky AS. Injurious ventilatory strategies increase cytokines and c-fos m-RNA expression in an isolated rat lung model. J Clin Invest. Mar 1; 1997 99(5):944–52. [PubMed: 9062352]

[5]. Villar J, Flores C, Mendez-Alvarez S. Genetic susceptibility to acute lung injury. Crit Care Med. Apr; 2003 31(4 Suppl):S272–5. [PubMed: 12682452]

[6]. Nonas S, Birukova AA, Fu P, Xing J, Chatchavalvanich S, Bochkov VN, et al. Oxidized phospholipids reduce ventilator-induced vascular leak and inflammation in vivo. Crit Care. Feb 27.2008 12(1):R27. [PubMed: 18304335]

[7]. Quinn DA, Moufarrej RK, Volokhov A, Hales CA. Interactions of lung stretch, hyperoxia, and MIP-2 production in ventilator-induced lung injury. J Appl Physiol. Aug; 2002 93(2):517–25. [PubMed: 12133859]

[8]. Finigan JH, Boueiz A, Wilkinson E, Damico R, Skirball J, Pae HH, et al. Activated protein C protects against ventilator-induced pulmonary capillary leak. Am J Physiol Lung Cell Mol Physiol. Jun; 2009 296(6):L1002–11. [PubMed: 19363121]

[9]. Boueiz A, Hassoun PM. Regulation of endothelial barrier function by reactive oxygen and nitrogen species. Microvasc Res. Jan; 2009 77(1):26–34. [PubMed: 19041330]

[10]. Tasaka S, Amaya F, Hashimoto S, Ishizaka A. Roles of oxidants and redox signaling in the pathogenesis of acute respiratory distress syndrome. Antioxid Redox Signal. Apr; 2008 10(4): 739–53. [PubMed: 18179359]

[11]. Ali MH, Pearlstein DP, Mathieu CE, Schumacker PT. Mitochondrial requirement for endothelial responses to cyclic strain: implications for mechanotransduction. Am J Physiol Lung Cell Mol Physiol. Sep; 2004 287(3):L486–96. [PubMed: 15090367]

[12]. Grote K, Flach I, Luchtefeld M, Akin E, Holland SM, Drexler H, et al. Mechanical stretch enhances mRNA expression and proenzyme release of matrix metalloproteinase-2 (MMP-2) via NAD(P)H oxidase-derived reactive oxygen species. Circ Res. Jun 13; 2003 92(11):e80–6. [PubMed: 12750313]

[13]. Abdulnour RE, Peng X, Finigan JH, Han EJ, Hasan EJ, Birukov KG, et al. Mechanical stress activates xanthine oxidoreductase through MAP kinase-dependent pathways. Am J Physiol Lung Cell Mol Physiol. Sep; 2006 291(3):L345–53. [PubMed: 16632522]

[14]. Chapman KE, Sinclair SE, Zhuang D, Hassid A, Desai LP, Waters CM. Cyclic mechanical strain increases reactive oxygen species production in pulmonary epithelial cells. Am J Physiol Lung Cell Mol Physiol. Nov; 2005 289(5):L834–41. [PubMed: 15964900]

[15]. Chess PR, Toia L, Finkelstein JN. Mechanical strain-induced proliferation and signaling in pulmonary epithelial H441 cells. Am J Physiol Lung Cell Mol Physiol. 2000; 279(1):L43–51. [PubMed: 10893201]

[16]. Papaiahgari S, Yerrapureddy A, Hassoun PM, Garcia JG, Birukov KG, Reddy SP. EGFR-activated signaling and actin remodeling regulate cyclic stretch-induced NRF2-ARE activation. Am J Respir Cell Mol Biol. Mar; 2007 36(3):304–12. [PubMed: 17008637]

[17]. Birukov KG. Cyclic stretch, reactive oxygen species and vascular remodeling. Antioxid Redox Signal. Feb 2; 2009 11(7):1651–67. [PubMed: 19186986]

[18]. Comhair SA, Erzurum SC. Antioxidant responses to oxidant-mediated lung diseases. Am J Physiol Lung Cell Mol Physiol. Aug; 2002 283(2):L246–55. [PubMed: 12114185]

[19]. Comhair SA, Xu W, Ghosh S, Thunnissen FB, Almasan A, Calhoun WJ, et al. Superoxide dismutase inactivation in pathophysiology of asthmatic airway remodeling and reactivity. Am J Pathol. Mar; 2005 166(3):663–74. [PubMed: 15743779]

[20]. Epperly MW, Epstein CJ, Travis EL, Greenberger JS. Decreased pulmonary radiation resistance of manganese superoxide dismutase (MnSOD)-deficient mice is corrected by human manganese superoxide dismutase-Plasmid/Liposome (SOD2-PL) intratracheal gene therapy. Radiat Res. Oct; 2000 154(4):365–74. [PubMed: 11023599]

[21]. Asikainen TM, Huang TT, Taskinen E, Levonen AL, Carlson E, Lapatto R, et al. Increased sensitivity of homozygous Sod2 mutant mice to oxygen toxicity. Free Radic Biol Med. Jan 15; 2002 32(2):175–86. [PubMed: 11796207]

[22]. Arita Y, Harkness SH, Kazzaz JA, Koo HC, Joseph A, Melendez JA, et al. Mitochondrial localization of catalase provides optimal protection from H2O2-induced cell death in lung epithelial cells. Am J Physiol Lung Cell Mol Physiol. May; 2006 290(5):L978–86. [PubMed: 16387755]

[23]. Nowak K, Weih S, Metzger R, Albrecht RF 2nd, Post S, Hohenberger P, et al. Immunotargeting of catalase to lung endothelium via anti-angiotensin-converting enzyme antibodies attenuates ischemia-reperfusion injury of the lung in vivo. Am J Physiol Lung Cell Mol Physiol. Jul; 2007 293(1):L162–9. [PubMed: 17435080]

[24]. Smoluk GD, Fahey RC, Calabro-Jones PM, Aguilera JA, Ward JF. Radioprotection of cells in culture by WR-2721 and derivatives: form of the drug responsible for protection. Cancer Res. Jul 1; 1988 48(13):3641–7. [PubMed: 2837320]

[25]. Brizel DM, Wasserman TH, Henke M, Strnad V, Rudat V, Monnier A, et al. Phase III randomized trial of amifostine as a radioprotector in head and neck cancer. J Clin Oncol. Oct 1; 2000 18(19):3339–45. [PubMed: 11013273]

[26]. Fu P, Birukova AA, Xing J, Sammani S, Murley JS, Garcia JG, et al. Amifostine reduces lung vascular permeability via suppression of inflammatory signalling. Eur Respir J. Mar; 2009 33(3): 612–24. [PubMed: 19010997]

[27]. Grdina DJ, Murley JS, Kataoka Y, Baker KL, Kunnavakkam R, Coleman MC, et al. Amifostine induces antioxidant enzymatic activities in normal tissues and a transplantable tumor that can affect radiation response. Int J Radiat Oncol Biol Phys. Mar 1; 2009 73(3):886–96. [PubMed: 19215822]

[28]. Dragojevic-Simic VM, Dobric SL, Bokonjic DR, Vucinic ZM, Sinovec SM, Jacevic VM, et al. Amifostine protection against doxorubicin cardiotoxicity in rats. Anticancer Drugs. Feb; 2004 15(2):169–78. [PubMed: 15075674]

[29]. Birukova AA, Fu P, Xing J, Birukov KG. Rap1 mediates protective effects of iloprost against ventilator induced lung injury. J Appl Physiol. Oct 22; 2009 107(6):1900–10. [PubMed: 19850733]

[30]. Birukova AA, Fu P, Xing J, Yakubov B, Cokic I, Birukov KG. Mechanotransduction by GEF-H1 as a novel mechanism of ventilator-induced vascular endothelial permeability. Am J Physiol Lung Cell Mol Physiol. Jun; 2010 298(6):L837–48. [PubMed: 20348280]

[31]. Singleton PA, Chatchavalvanich S, Fu P, Xing J, Birukova AA, Fortune JA, et al. Akt-mediated transactivation of the S1P1 receptor in caveolin-enriched microdomains regulates endothelial barrier enhancement by oxidized phospholipids. Circ Res. Apr 24; 2009 104(8):978–86. [PubMed: 19286607]

[32]. Nonas SA, Miller I, Kawkitinarong K, Chatchavalvanich S, Gorshkova I, Bochkov VN, et al. Oxidized phospholipids reduce vascular leak and inflammation in rat model of acute lung injury. Am J Respir Crit Care Med. May 15; 2006 173(10):1130–8. [PubMed: 16514111]

[33]. Birukova AA, Fu P, Xing J, Cokic I, Birukov KG. Lung endothelial barrier protection by iloprost in the 2-hit models of ventilator-induced lung injury (VILI) involves inhibition of Rho signaling. Transl Res. Jan; 2010 155(1):44–54. [PubMed: 20004361]

[34]. Moitra J, Sammani S, Garcia JG. Re-evaluation of Evans Blue dye as a marker of albumin clearance in murine models of acute lung injury. Transl Res. Oct; 2007 150(4):253–65. [PubMed: 17900513]

[35]. Birukov KG, Jacobson JR, Flores AA, Ye SQ, Birukova AA, Verin AD, et al. Magnitude-dependent regulation of pulmonary endothelial cell barrier function by cyclic stretch. Am J Physiol Lung Cell Mol Physiol. Oct; 2003 285(4):L785–97. [PubMed: 12639843]

[36]. Birukova AA, Rios A, Birukov KG. Long-term cyclic stretch controls pulmonary endothelial permeability at translational and post-translational levels. Experimental cell research. Nov 15; 2008 314(19):3466–77. [PubMed: 18824167]

[37]. Birukova AA, Chatchavalvanich S, Rios A, Kawkitinarong K, Garcia JG, Birukov KG. Differential regulation of pulmonary endothelial monolayer integrity by varying degrees of cyclic stretch. Am J Pathol. May; 2006 168(5):1749–61. [PubMed: 16651639]

[38]. Birukova AA, Moldobaeva N, Xing J, Birukov KG. Magnitude-dependent effects of cyclic stretch on HGF- and VEGF-induced pulmonary endothelial remodeling and barrier regulation. Am J Physiol Lung Cell Mol Physiol. Aug 8; 2008 295(4):L612–23. [PubMed: 18689603]

[39]. Reddy SP, Hassoun PM, Brower R. Redox imbalance and ventilator-induced lung injury. Antioxid Redox Signal. Nov; 2007 9(11):2003–12. [PubMed: 17822361]

[40]. Matthay MA, Zimmerman GA, Esmon C, Bhattacharya J, Coller B, Doerschuk CM, et al. Future research directions in acute lung injury: summary of a National Heart, Lung, and Blood Institute working group. Am J Respir Crit Care Med. Apr 1; 2003 167(7):1027–35. [PubMed: 12663342]

[41]. Ichimura H, Parthasarathi K, Quadri S, Issekutz AC, Bhattacharya J. Mechano-oxidative coupling by mitochondria induces proinflammatory responses in lung venular capillaries. J Clin Invest. Mar; 2003 111(5):691–9. [PubMed: 12618523]

[42]. Ali MH, Mungai PT, Schumacker PT. Stretch-induced phosphorylation of focal adhesion kinase in endothelial cells: role of mitochondrial oxidants. Am J Physiol Lung Cell Mol Physiol. Jul; 2006 291(1):L38–45. [PubMed: 16510472]

[43]. Chandel NS, Budinger GR. The cellular basis for diverse responses to oxygen. Free Radic Biol Med. Jan 15; 2007 42(2):165–74. [PubMed: 17189822]

[44]. Goldberg PL, MacNaughton DE, Clements RT, Minnear FL, Vincent PA. p38 MAPK activation by TGF-beta1 increases MLC phosphorylation and endothelial monolayer permeability. Am J Physiol Lung Cell Mol Physiol. Jan; 2002 282(1):L146–54. [PubMed: 11741826]

[45]. Kevil CG, Oshima T, Alexander JS. The role of p38 MAP kinase in hydrogen peroxide mediated endothelial solute permeability. Endothelium. 2001; 8(2):107–16. [PubMed: 11572474]

[46]. Niwa K, Inanami O, Ohta T, Ito S, Karino T, Kuwabara M. p38 MAPK and Ca2+ contribute to hydrogen peroxide-induced increase of permeability in vascular endothelial cells but ERK does not. Free Radic Res. Nov; 2001 35(5):519–27. [PubMed: 11767410]

[47]. Shaw LM, Bonner HS, Schuchter L, Schiller J, Lieberman R. Pharmacokinetics of amifostine: effects of dose and method of administration. Semin Oncol. Apr; 1999 26(2 Suppl 7):34–6. [PubMed: 10348258]

[48]. Fan M, Ahmed KM, Coleman MC, Spitz DR, Li JJ. Nuclear factor-kappaB and manganese superoxide dismutase mediate adaptive radioresistance in low-dose irradiated mouse skin epithelial cells. Cancer Res. Apr 1; 2007 67(7):3220–8. [PubMed: 17409430]

[49]. Murley JS, Kataoka Y, Hallahan DE, Roberts JC, Grdina DJ. Activation of NFkappaB and MnSOD gene expression by free radical scavengers in human microvascular endothelial cells. Free Radic Biol Med. Jun 15; 2001 30(12):1426–39. [PubMed: 11390188]

[50]. Murley JS, Kataoka Y, Weydert CJ, Oberley LW, Grdina DJ. Delayed cytoprotection after enhancement of Sod2 (MnSOD) gene expression in SA-NH mouse sarcoma cells exposed to WR-1065, the active metabolite of amifostine. Radiat Res. Jul; 2002 158(1):101–9. [PubMed: 12071809]

[51]. Xu Y, Kiningham KK, Devalaraja MN, Yeh CC, Majima H, Kasarskis EJ, et al. An intronic NF-kappaB element is essential for induction of the human manganese superoxide dismutase gene by tumor necrosis factor-alpha and interleukin-1beta. DNA Cell Biol. Sep; 1999 18(9):709–22. [PubMed: 10492402]

[52]. Kops GJ, Dansen TB, Polderman PE, Saarloos I, Wirtz KW, Coffer PJ, et al. Forkhead transcription factor FOXO3a protects quiescent cells from oxidative stress. Nature. Sep 19; 2002 419(6904):316–21. [PubMed: 12239572]

[53]. Murley JS, Kataoka Y, Cao D, Li JJ, Oberley LW, Grdina DJ. Delayed radioprotection by NFkappaB-mediated induction of Sod2 (MnSOD) in SA-NH tumor cells after exposure to clinically used thiol-containing drugs. Radiat Res. Nov; 2004 162(5):536–46. [PubMed: 15624308]

[54]. Matthews JR, Wakasugi N, Virelizier JL, Yodoi J, Hay RT. Thioredoxin regulates the DNA binding activity of NF-kappa B by reduction of a disulphide bond involving cysteine 62. Nucleic Acids Res. Aug 11; 1992 20(15):3821–30. [PubMed: 1508666]

[55]. Kataoka Y, Murley JS, Khodarev NN, Weichselbaum RR, Grdina DJ. Activation of the nuclear transcription factor kappaB (NFkappaB) and differential gene expression in U87 glioma cells after exposure to the cytoprotector amifostine. Int J Radiat Oncol Biol Phys. May 1; 2002 53(1): 180–9. [PubMed: 12007958]

[56]. Grdina DJ, Kataoka Y, Murley JS, Swedberg K, Lee JY, Hunter N, et al. Antimetastatic effectiveness of amifostine therapy following surgical removal of Sa-NH tumors in mice. Semin Oncol. Dec; 2002 29(6 Suppl 19):22–8. [PubMed: 12577239]

[57]. Koukourakis MI, Giatromanolaki A, Chong W, Simopoulos C, Polychronidis A, Sivridis E, et al. Amifostine induces anaerobic metabolism and hypoxia-inducible factor 1 alpha. Cancer Chemother Pharmacol. Jan; 2004 53(1):8–14. [PubMed: 14574457]

[58]. Dedieu S, Canron X, Rezvani HR, Bouchecareilh M, Mazurier F, Sinisi R, et al. The cytoprotective drug amifostine modifies both expression and activity of the pro-angiogenic factor VEGF-A. BMC Med. 2010; 8:19. [PubMed: 20334641]

[59]. Mura M, Han B, Andrade CF, Seth R, Hwang D, Waddell TK, et al. The early responses of VEGF and its receptors during acute lung injury: implication of VEGF in alveolar epithelial cell survival. Crit Care. 2006; 10(5):R130. [PubMed: 16968555]

[60]. Karmpaliotis D, Kosmidou I, Ingenito EP, Hong K, Malhotra A, Sunday ME, et al. Angiogenic growth factors in the pathophysiology of a murine model of acute lung injury. Am J Physiol Lung Cell Mol Physiol. Sep; 2002 283(3):L585–95. [PubMed: 12169578]

[61]. Vlahakis NE, Hubmayr RD. Invited review: plasma membrane stress failure in alveolar epithelial cells. J Appl Physiol. 2000; 89(6):2490–6. discussion 7. [PubMed: 11090606]

[62]. Frank JA, Matthay MA. Science review: mechanisms of ventilator-induced injury. Crit Care. Jun; 2003 7(3):233–41. [PubMed: 12793874]

[63]. Schultz MJ, Haitsma JJ, Zhang H, Slutsky AS. Pulmonary coagulopathy as a new target in therapeutic studies of acute lung injury or pneumonia--a review. Crit Care Med. Mar; 2006 34(3): 871–7. [PubMed: 16521285]

[64]. Maniatis NA, Kotanidou A, Catravas JD, Orfanos SE. Endothelial pathomechanisms in acute lung injury. Vascul Pharmacol. Oct-Dec;2008 49(4-6):119–33. [PubMed: 18722553]

[65]. Yun JK, Anderson JM, Ziats NP. Cyclic-strain-induced endothelial cell expression of adhesion molecules and their roles in monocyte-endothelial interaction. J Biomed Mater Res. 1999; 44(1): 87–97. [PubMed: 10397908]

[66]. Cheng JJ, Wung BS, Chao YJ, Wang DL. Cyclic strain-induced reactive oxygen species involved in ICAM-1 gene induction in endothelial cells. Hypertension. Jan; 1998 31(1):125–30. [PubMed: 9449403]

[67]. Metzler SA, Pregonero CA, Butcher JT, Burgess SC, Warnock JN. Cyclic strain regulates pro-inflammatory protein expression in porcine aortic valve endothelial cells. J Heart Valve Dis. Sep; 2008 17(5):571–7. discussion 8. [PubMed: 18980092]

[68]. Birukova AA, Burdette D, Moldobaeva N, Xing J, Fu P, Birukov KG. Rac GTPase is a hub for protein kinase A and Epac signaling in endothelial barrier protection by cAMP. Microvasc Res. Mar; 2010 79(2):128–38. [PubMed: 19962392]

[69]. Waters CM. Reactive oxygen species in mechanotransduction. Am J Physiol Lung Cell Mol Physiol. Sep; 2004 287(3):L484–5. [PubMed: 15308497]

[70]. Birukov KG, Bochkov VN, Birukova AA, Kawkitinarong K, Rios A, Leitner A, et al. Epoxycyclopentenone-containing oxidized phospholipids restore endothelial barrier function via Cdc42 and Rac. Circ Res. Oct 29; 2004 95(9):892–901. [PubMed: 15472119]

[71]. Kouklis P, Konstantoulaki M, Vogel S, Broman M, Malik AB. Cdc42 regulates the restoration of endothelial barrier function. Circ Res. Feb 6; 2004 94(2):159–66. [PubMed: 14656933]

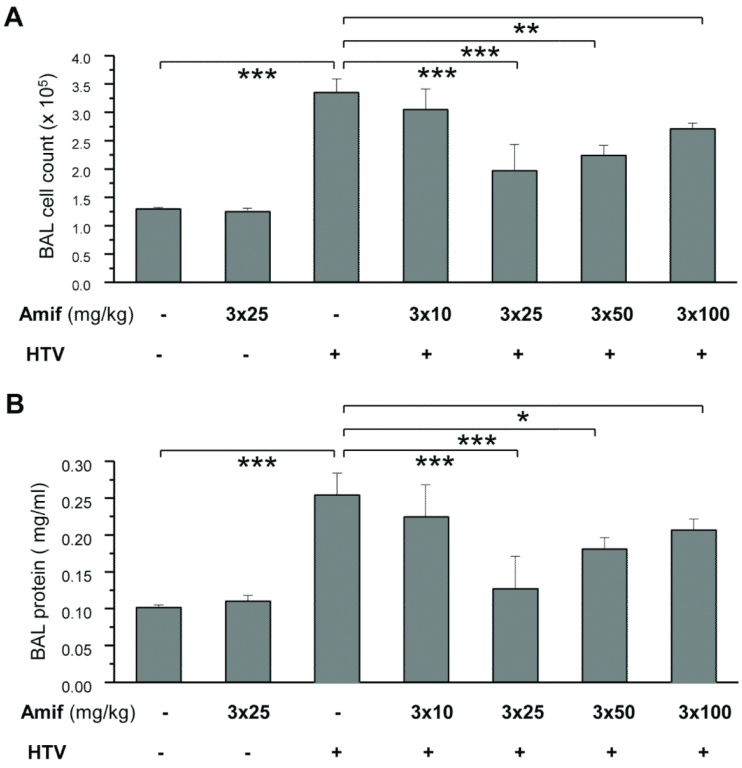

Figure 1. Chronic amifostine preconditioning attenuates high tidal volume ventilation-induced lung injury

A and B - Mice were pretreated with amifostine for 3 days followed by ventilation at HTV. Control animals were treated with vehicle (PBS) or amifostine alone. Cell count (**A**) and protein concentration (**B**) were measured in bronchoalveolar lavage fluid taken from control and experimental animals. Data are presented as mean ± SD; n=4 in vehicle and amifostine groups; n=5 in groups of amifostine + HTV; n=10 in HTV group; *p<0.05, **p<0.01, ***p<0.001.

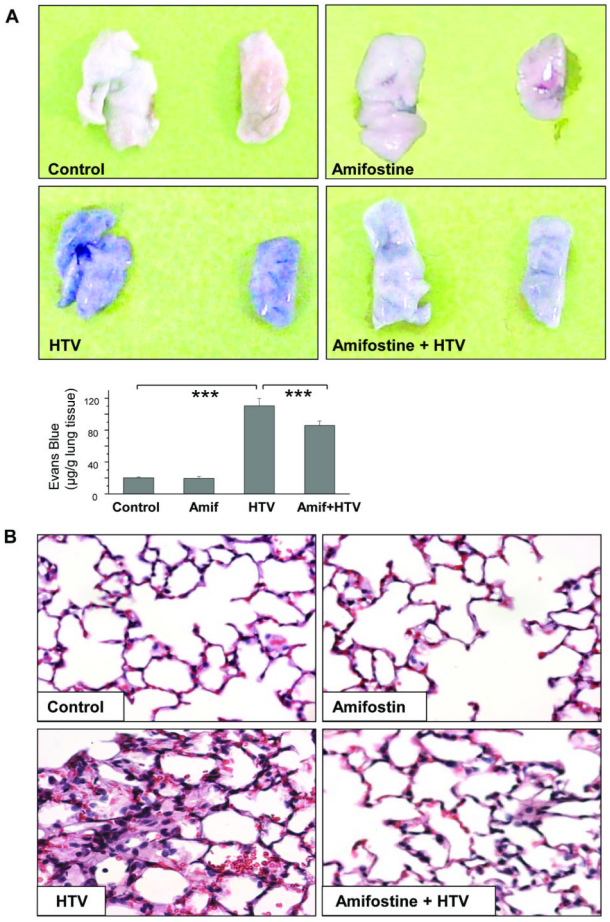

Figure 2. Chronic amifostine preconditioning alleviates lung vascular permeability and cellular infiltration induced by high tidal volume mechanical ventilation

Mice were pretreated with vehicle or amifostine (25 mg/kg) for 3 days followed by ventilation at HTV. Control animals were treated with vehicle (PBS) or amifostine alone. **A** - Lung vascular permeability was assessed by Evans blue accumulation in the lungs. The panels show right and left lungs respectively, which were excised after perfusion to remove blood and imaged. Bar graph depicts quantitative spectrophotomertic analysis of Evans blue-labeled albumin content in the lung tissues. Data are presented as mean ± SD; n=4-6 mice per group; ***p<0.001. **B** - Lung specimen from control and experimental animals were stained with hematoxylin and eosin. Images are representative of 4-6 lung specimen for each condition; ×40 magnification.

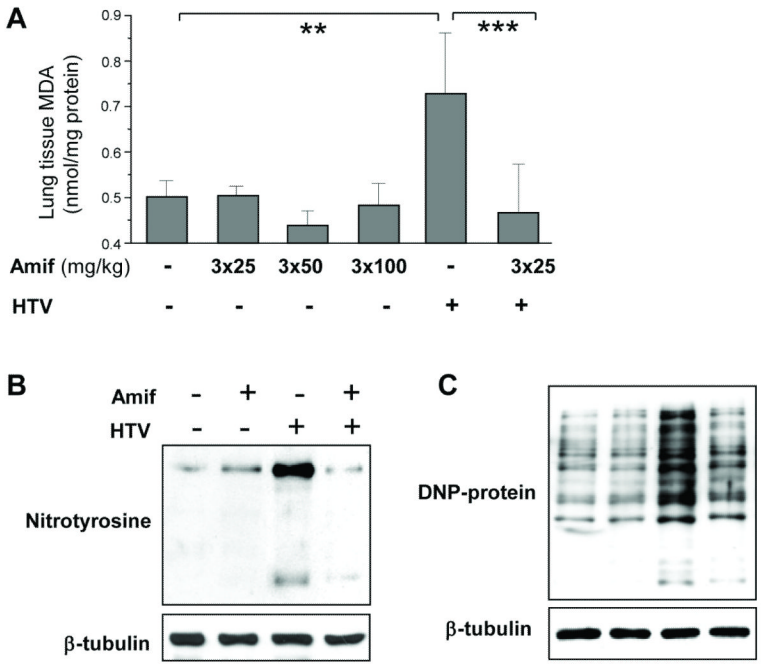

Figure 3. Amifostine attenuates lung oxidative stress by HTV

A - Measurements of malone dialdehyde (MDA) content in control and HTV-exposed lungs with or without amifostine preconditioning. Data are presented as mean ± SD; n=4 in vehicle group; n=6 in the other groups; **p<0.01, ***p<0.001. **B** - levels of nitrotyrosinated proteins, and **C** - DNP-derivatized oxidized proteins in lung tissue samples as indices of oxidative stress were analyzed by western blot in control and amifostine-peconditioned (25 mg/kg, three daily i.p. injections) lungs after HTV exposure. Shown are representative results of 5 experiments.

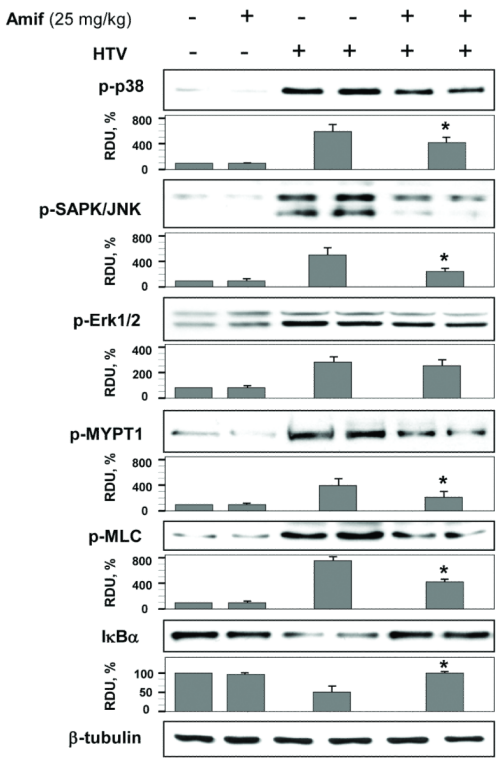

Figure 4. Amifostine inhibits HTV-induced MAP kinase signaling and IκBα degradation in mouse lungs

Lungs from control or amifostine-preconditioned (25 mg/kg, three daily i.p. injections) mice were subjected to HTV. Control animals were treated with vehicle (PBS) or amifostine alone. Phosphorylation of p38, JNK, Erk-1,2, MYPT and MLC, and degradation of IκBα in tissue samples was analyzed by western blot. Tissue samples from HTV-exposed animals with and without amifostine pretreatment are presented in duplicates. Equal protein loading was confirmed by probing of membranes with β-tubulin antibodies. Results of densitometry normalized to β-tubulin signal are shown as mean±SD; n=6 per condition. Bars depict marker phospho-protein levels in tissue samples corresponding to control group without amifostine pretreatment; HTV; and HTV+amifostine groups. *$p<0.05$ as compared to HTV.

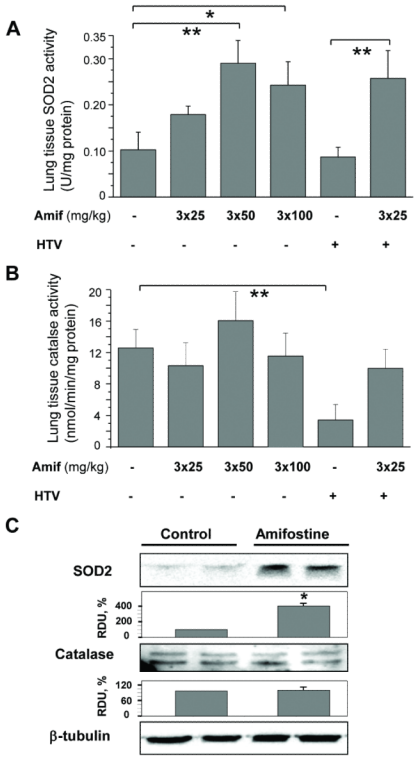

Figure 5. Effect of amifostine on the enzyme activities of SOD and catalse and their expression in lung tissue

Mice were pretreated with vehicle (PBS) or amifostine for 3 days followed by ventilation at HTV. **A and B** - Measurements of SOD (**A**) or catalase (**B**) activity. Data are presented as mean ± SD; n=4-6 mice per each dose group; *p<0.05, **p<0.01. **C** - Protein expression of SOD2 and catalase in control and amifostine-preconditioned lungs was analyzed by western blot of tissue samples. The expression levels of each protein was quantified by densitometry and normalized to β-tubulin signal. Tissue samples are presented in duplicates. Results shown as mean±SD; n=6 for each group; *p<0.05.

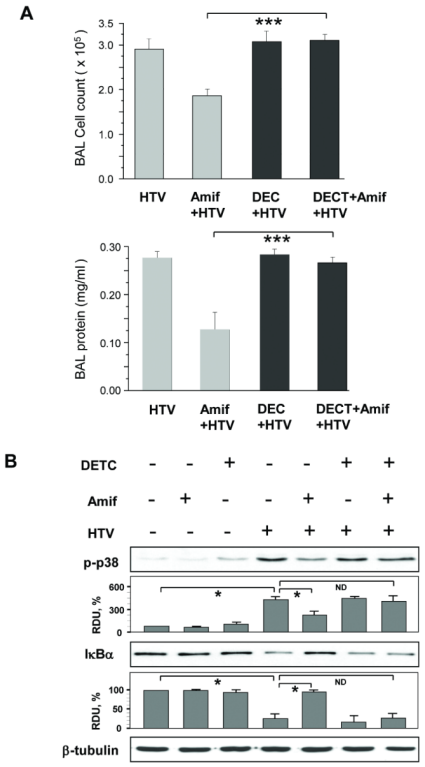

Figure 6. SOD inhibitor DECT relieves protective effect of amifostine against HTV-induced lung injury and blocking of HTV-induced stress signaling

Mice were preconditioned with amifostine (25 mg/kg, three daily injections) with or without DETC injection prior to HTV. Control animals were treated with vehicle (PBS). **A** - Measurements of cell counts and protein content in BAL samples. Values are mean ± SD, n=4 for each group; ***p<0.001. **B** - Phosphorylation of p38 MAP kinase and degradation of IκBα was analyzed by western blot and quantified by densitometry. Results of densitometry shown as mean±SD; n=4 for each group; *p<0.05.

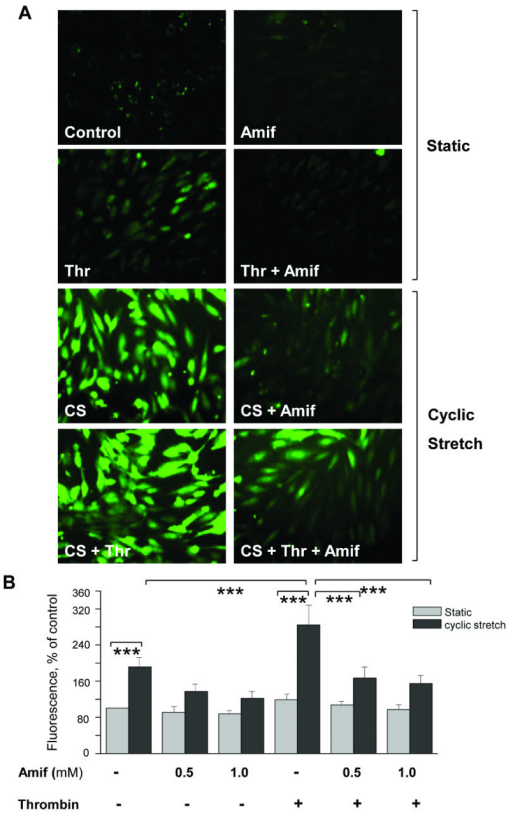

Figure 7. Amifostine inhibits cyclic stretch- and thrombin-induced ROS production in human pulmonary EC

Control and amifostine-preconditioned (Amif) HPAEC grown on BioFlex plates were exposed to 18% cyclic stretch (CS) followed by thrombin (Thr) stimulation or left under static conditions. To detect ROS, 30 min prior to termination of the experiment cells were incubated with fluorescent dye for ROS, dichlorodihydrofluorescein (DCFDA, 10 μM) under continuing CS stimulation. **A** -Cells were imaged using inverted fluorescent microscope. **B** - Fluorescence intensity determined in vehicle control cells was taken as 100%. Results of 6 images from the entire cell monolayer were averaged and have been reproduced in 3 independent experiments. Results are presented as mean ± SD; ***p<0.001.

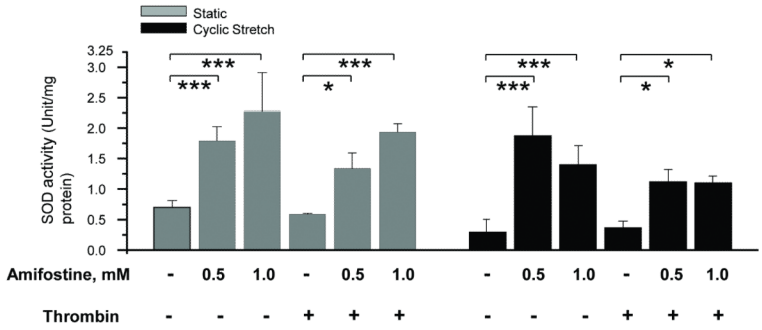

Figure 8. Amifostine pretreatment increases SOD activity in human pulmonary endothelial cells

HPAEC were pretreated with vehicle (PBS) or amifostine for 3 days followed by 18% CS with or without thrombin challenge. Control cells were left under static conditions. Measurements of SOD activity were performed in control and stimulated cells. Data are presented as mean ± SD; n=3 for each group; *p<0.05; ***p<0.001.

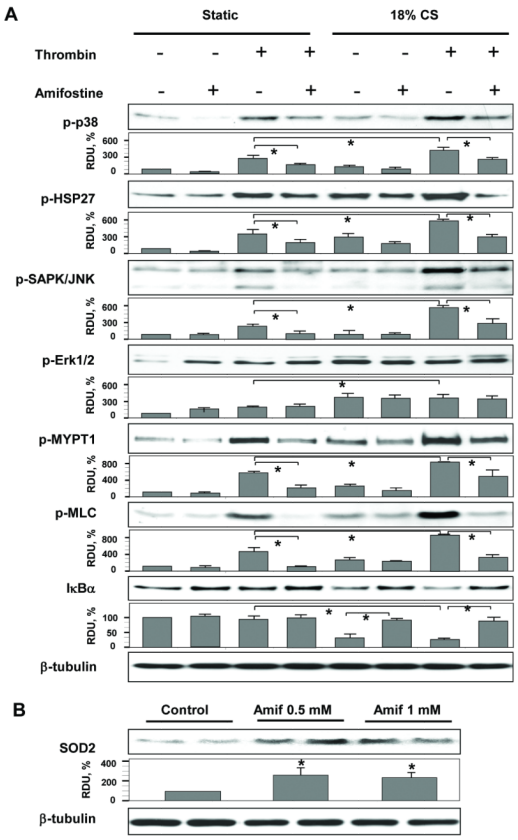

Figure 9. Amifostine pretreatment attenuates cyclic stretch- and thrombin-induced activation of stress cascades and barrier disruptive signaling

HPAEC were preconditioned with vehicle (PBS) or amifostine followed by 18% CS with or without thrombin treatment, or left static. **A** - Effect of amifostine preconditioning on activation of oxidative stress sensitive pathways was analyzed by western blot with specific antibodies and quantitative densitometry analysis. Results of densitometry shown as mean ±SD; n=4 for each group; *p<0.05. **B** - SOD2 expression levels in HPAEC were quantified by densitometry and normalized to β-tubulin. Results shown as mean±SD; n=6 for each group; *p<0.05.

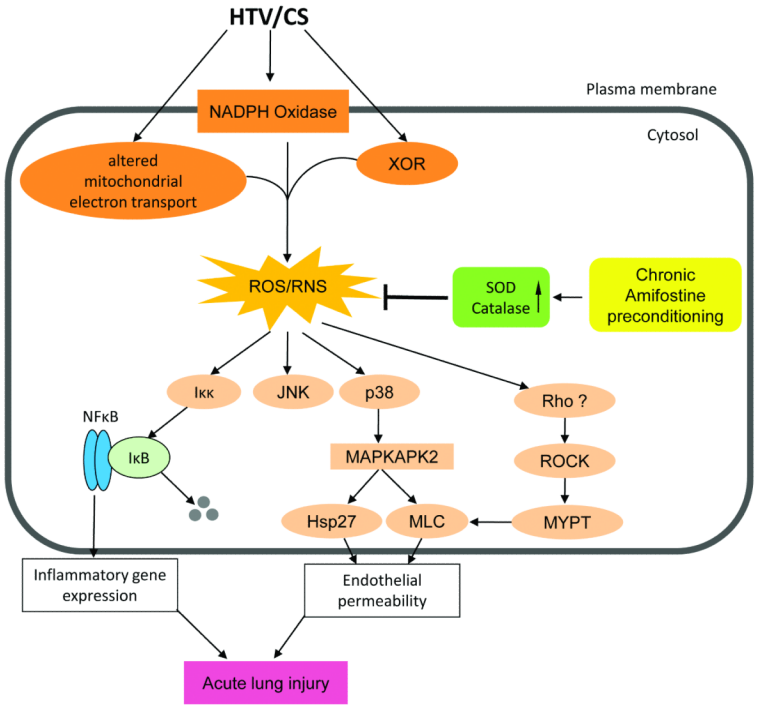

Figure 10. Attenuation of ventilator induced lung injury by amifostine

Mechanical stretch associated with high tidal volume mechanical ventilation induces reactive oxygen species (ROS) and reactive nitrogen species (RNS) production, leading to activation of redox-sensitive stress kinases (JNK and p38 MAPK) and NFkB signaling cascade leading to expression of pro-inflammatory cytokines, cytoskeletal remodeling and disruption of endothelial monolayer integrity. Amifostine attenuates oxidative stress induced by HTV through upregulation of SOD protein expression and stimulation of SOD and catalase enzymatic activities. XOR – xanthine oxidoreductase; SOD – superoxide dismutase; MAPKAPK2 – MAPK-activated protein kinase 2 ; Hsp27 – heat shock protein 27; MLC – myosin light chains; ROCK – Rho associated kinase; MYPT – myosin protein phosphatase.